Applied Physics A (2021) 127:726
https://doi.org/10.1007/s00339-021-04880-4

Applied Physics A
Materials Science & Processing

Investigation of N + SiGe juntionless vertical TFET with gate stack for gas sensing application

Shailendra Singh[1] · Abhishek Sharma[2] · Vikrant Kumar[2] · Pallavi Umar[2] · Ashish Kumar Rao[2] · Arun Kumar Singh[2]

Received: 8 May 2021 / Accepted: 24 August 2021 / Published online: 31 August 2021
© The Author(s), under exclusive licence to Springer-Verlag GmbH, DE part of Springer Nature 2021

Abstract

In this work, a novel N + SiGe delta-doped gate stacked junctionless vertical tunnel field transistor (N + SiGe gate staked JL-VTFET) is proposed and investigated with its electrical characteristics for gas sensing application using the Silvaco TCAD simulation software. This vertical distribution of the source, channel, and drain will enhance the stability of the device. The integrated effects of vertical tunneling as compared to lateral tunneling will enhance the device sensitivity and decrease the subthreshold slope. The gate stacking of High-K (HfO_2) with (SiO_2) and the two-side gate metal electrode makes a good electrostatic control over a proposed device. Also, the presence of SiGe layer in between the source-channel interface will lead to the decrease in the tunneling barrier and enhance the device performance by reducing the energy bandgap from 1.1 eV to 0.7 eV. This paper analyses hydrogen gas using palladium and ammonia gas using Cobalt and Molybdenum metals as a gate electrode. Utilizing work function values appropriate for the above metals, p + regions are generated close to the source field. By using the Silvaco ATLAS TCAD simulator, the proposed structure's characteristics are investigated using the surface potential, electric field and energy bandgap diagrams for gas molecule adsorption on metal surface. The reported sensitivity ($\sim S_{Idoff}$) is higher for the lower work function for Molybdenum, Cobalt and Palladium is 8.89×10^2, 2.04×10^3 and 1.97×10^3 with high I_{don}/I_{doff} current ratio ($\sim 6.4 \times 10^4$, 9.45×10^7, 1.1×10^{11}), respectively.

Keywords Junctionless vertical tunnel field-effect transistor (JL-VTEFT) · Subthreshold slope (SS) · BTBT (Band-to-Band Tunneling) · Gas sensing · Gate stacking · SiGe heterojunction · Work function variation (WFV)

1 Introduction

The very large-scale integration (VLSI) industry is looking into devices that consume ultra-low power and do great work at the nanoscale in the era of fabricating devices with high packaging density, and its sensitivity is feasible with the recent technology. After Moore's Law, the international technology roadmap for semiconductors (ITRS) came out for the technology assessment in order to measure the packaging density and reduction in the short channel effect [1, 2]. In the past few decades, the semiconductor industry has been growing rapidly on the three-basic fundamentals: optimizing performance, low-cost fabrication, and technology scaling for low-power devices [3, 4]. However, nanodevice scaling will cause the short channel effects like drain-induced barrier lowering (DIBL), hot electron effect which still degrades the performance of lower power applications [5]. Although, the metal oxide semiconductor field-effect transistor (MOSFET) still limits to 60 mV/dec for its subthreshold slope (SS) [6]. As a substitute, many of the nanoscale devices come up with their various advantages, among which, the tunnel field-effect transistor (TFET) came out to be the most promising emerging device in terms of fabrication complexity and manufacturing cost [7]. The TFET has the p-i-n diode structure whose working principle is based upon the band-to-band tunneling mechanism. It has come up over all the short channel effects with a very low subthreshold slope and leakage current [8–10].

Because high doping concentration at nanoscale regime becomes a challenge due to the effect of Radom doping fluctuation, which overall increases the cost of packaging due to involvement of diffusion process and ion-implantation method for precise coating [11]. With respect to the above issue, a new transistor design known to be junctionless filed

✉ Shailendra Singh
shailendras.nitj@gmail.com

[1] ECE, PSIT, Kanpur, India

[2] Department of Electronics Engineering, REC, Kannauj, India

effect transistor (JTFET) is introduced as a substitute in the coming era of devices. Unlike the conventional TFET, junctionless TFET has no metallurgical junction and has uniform doping throughout the device, i.e., source, channel, and drain. Due to this, the device becomes inexpensive as there is no requirement of the ion-implantation method and above heavy diffusion technology [12]. However, arranging the device fabrication in the vertical direction will increase the scalability of the device. With the J-VTFET, it has been reported with the high switching speed and overcomes the limitation of 60 mV/dec subthreshold slope over the Metal oxide semiconductor field-effect transistor (MOSFET) device [13, 14].

Now coming to the application section, some of follow up research based on TFET sensor have been taken on record. Using the Sol–Gel process, many of the solutions have been prepared to cope over the ITO film and sense the gas chamber and find out the change in resistance sensitivity with gas and without gas sensing material [15]. However, when it comes to device engineering based on novel architectures, variations of different gas can be sensed with respect to the variations in the work function. The BTBT tunneling process, which regulates the flow of carriers and detects hazardous gaseous particles in the environment, is the fundamental principle behind TFET-based sensors. Fine, Wollenstein, Lopez, and others have used different architectures for ammonia gas sensing over the last decade [16–18]. Bjorn Timmer et al. have done detailed studies on the benefits of ammonia gas detection in comparison to solid-state ammonia detection [19]. As a result, very low amounts of any harmful substance (less than 2 ppb) are easier to detect in gas form in comparison to solid-state. This record assisted in the development of environmental scanners and breathe analyzers for patients. Tsukada, Gautam et al., and others have done similar research on hydrogen gas sensing [20, 21].

In this work, an N + SiGe delta-doped gate stacked junctionless vertical tunnel field transistor (N + SiGe gate staked JL-VTFET) is proposed and analyzed with its electrical characteristics for gas sensing application using the Silvaco TCAD simulation software [22, 23]. The device having uniform doping throughout the structure and differentiate the junctions by inducing different work function values. The fabrication process is easy since no metallurgical junction is necessary. Furthermore, uniform distributions in the tunneling direction result in better electrical properties with only minor differences. The device's short-channel effects are diminished due to the absence of sharp doping gradients. Since VTFETs are not limited by channel duration, they can go beyond 10 nm and gain from the reduced on-chip region. The current aggressive interface shrinking pattern necessitates a reduction in overall oxide-thickness, with effective-oxide-thickness (EOT) of SiO_2 of about 0.5 nm packed with HfO_2 of 3 nm. Due to thermal stability and low trap density, HfO_2 is a good choice for low-power nanoscale devices [24]. The lack of abrupt and abnormal junctions' source-channel and drain, when the doping concentration gradient element is eliminated, further simplifies the design of JL-VTFETs over traditional TFETs.

2 Device design and simulation setup

The 2D schematic diagram of JL-VTFET is depicted in Fig. 1. The device's width is contoured by the x-axis, and its length is contoured by the y-axis. SiO_2/HfO_2 mounted gate oxide is integrated bilaterally around the channel, replacing the traditional gate oxide. A silicon body with 1×10^{19} cm^{-3} doping of n-type and 50 nm channel length (L_{ch}) and 10 nm channel thickness (T_{ch}) is used to make the device junctionless. To build p + pockets, source electrodes were made of platinum metal contacts with a work function ($\phi ms = 5.93eV$). The main goal of the proposed geometrical design is to transform the device structure from (N + /N + /N +) to (p + /i/N +) structure. This can be done by varying the work function in order to induce the junction for source, channel, and drain, respectively. The device parameters used to form the structure are listed in Table 1. The proposed junction less vertical TFET device (JL-VTFET) has a delta layer of SiGe with a similar doping level as the silicon body, i.e., 1×10^{19} cm^{-3}. The optimized mole fraction for $Si_{1-x}Ge_x$ material is taken to be at $x = 0.8$, which means 80% of the germanium percentage has been taken at the source-channel interface. As a result, the tunneling barrier reduces from 1.1 to 0.7 eV and enhances the overall drain current and sensitivity of the device. The operating voltage of the device is taken to be

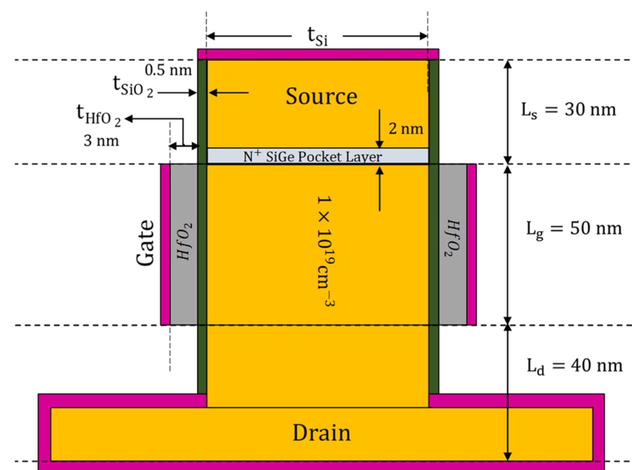

Fig. 1 Schematic diagram of a simulated N + SiGe delta-doped gate stacked junction less vertical tunnel field transistor (N + SiGe gate staked JL-VTFET)

Table 1 Selected device design specification of N + GS JL-VTFET

Parameter used	Specification (delta-doped N + GS JL-VTFET)
Gate oxide-thickness- SiO_2/ HfO_2	0.5 nm/ 3 nm
Silicon substrate doping (N_d)	1×10^{19} cm^{-3}
N + SiGe delta-doped Layer doping	1×10^{19} cm^{-3}
SiGe layer width	2 nm/10 nm
Body thickness (t_{si})	10 nm
Channel Length (T_{ch})	50 nm
Source doping work function	5.91 eV
V_{gs}/V_{ds} operating voltage	1 V/1 V
Length of Si Substrate	120 nm

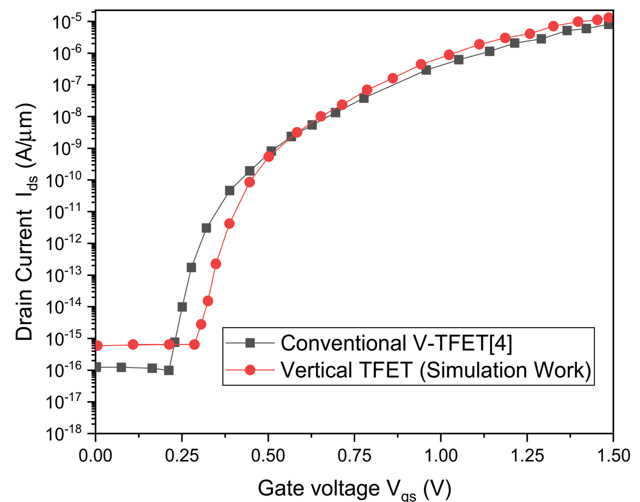

Fig. 2 Calibrated graph against experimental data of vertical TFET with conventional device

1 V for both gate-source (V_{gs}) and drain-source voltages (V_{ds}), respectively. Moreover, this paper deals with the sensing of hydrogen and ammonia gases. This can be done by employing highly reactive metals such as Molybdenum ($\Delta\phi_{m1} = 4.50 - 4.70eV$), Cobalt ($\Delta\phi_{m2} = 4.9 - 5.10eV$), and Palladium ($\Delta\phi_{m3} = 5.2 - 5.5eV$) as gate metals, respectively [25]. Gas sensors function by converting the concentrations of various gaseous molecules into standard electrical signals through the use of specific physical and chemical reactions. When hazardous gas molecules, such as hydrogen and ammonia, react with the surface of catalytic metals at the gate, it causes a modification in the gate's working function. Equation (1) depicts work function variations due to pernicious gas molecule adsorption.

$$\Delta\phi_m = cont - \left[\left(\frac{RT}{4F}\right) \times ln(P)\right] \tag{1}$$

where the term, R stands for the gas constant, T for absolute temperature, and F and P stands for Faraday's constant and partial pressure.

This shows that the proposed structure can perform a wide variety of tasks. This eliminates the need for external doping conditions and solves the problem of RDF. For analyzing the models of the developed system at the nanoscale stage, Fermi–Dirac function and bandgap narrowing are included to justify the effect of high doping. The concentration-mobility model has been employed to account for the low field mobilities at room temperature. Non-local band-to-band tunneling is used for optimizing the effect of quantum tunneling with SRH recombination model. This will account for the effect of trap charges at the semiconductor-oxide interface. And also, Shockey Reed Hall model recombination has been used to investigate the effect of doping and temperature on electron lifetime [26, 27]. The two-dimensional junctionless VTFET's replication boundaries and model properties are close to those of a standard VTFET except that the channel area is doped more heavily. The proposed system is tested using VTFET experimental data, as shown in Fig. 2, and the Plot Digitizer method is used to obtain data about the channel present. The Silvaco 2D-ATLAS tool was used to perform all of the vertical TFET calculations.

3 Validation of proposed device with the reference structure

For band-to-band tunneling, the vertical dual-gate design offers greater gate control than traditional designs (BTBT) [28]. Due to its reduced value of subthreshold slope (SS) and its strong ON-state current, this suggested system could be employed for gas sensing in various applications [29]. Design for N + SiGe delta-doped JL-VTFETs with Molybdenum (Mo) metal as gate contacts is analyzed for Ammonia gas sense compared to referenced structure [30]. Figure 3a shows the drain characteristics comparison for the metal Molybdenum as a gate metal electrode of both devices of (N + SiGe JL-VTFET) and referenced structure of vertical nanowire filed effect transistor (VNWFET). In comparison to previous research, the ON-state current for sensing ammonia gas is shown to be fairly high. As in contrast to earlier gas sensor designs, the sensitivity values for JT-VTFET-based sensors using Co, Mo, and Pd metals as gate contacts are much higher (The calculations for sensitivity are given in Tables 2, 3, 4). Tables 2, 3, and 4 $\Delta\phi_m$ represent the change in work function (ΔWF) of the gate metal electrode due to the presence of gas molecules.

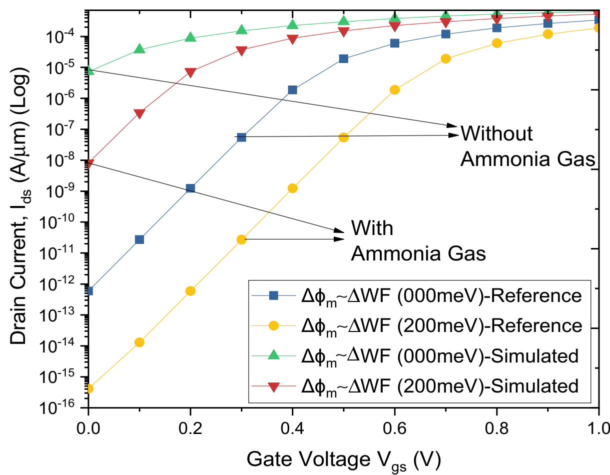

(a)

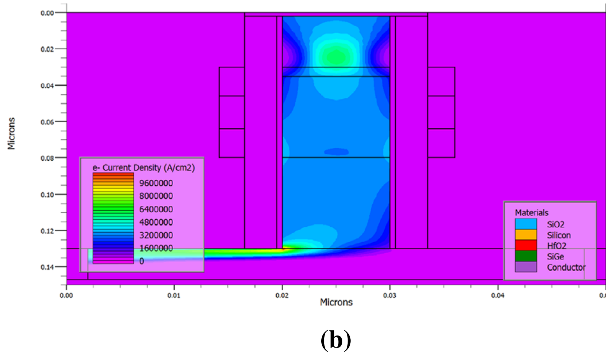

(b)

Fig. 3 **a** Comparison of drain characteristics for the metal Molybdenum as a gate metal electrode of proposed device with reference work [30]. **b** 2D contour plot of electron current density distribution of the N + SiGe gate staked JL-VTFET proposed device.

Table 2 Sensitivity calculation for molybdenum gate electrode for sensing ammonia gas

$\Delta\ \phi_m(meV)$	I_{doff}(A/μm)	I_{don}(A/μm)	I_{don}/I_{doff}	S_{doff}
Without gas	7.30E-06	0.000642	87.9653	1.00E+00
50	1.87E-06	0.000617	329.671	3.90E+00
100	3.42E-07	0.000589	1721.67	2.14E+01
150	5.41E-08	0.000558	10,318.1	1.35E+02
200	8.21E-09	0.000526	64,026.2	8.89E+02

Table 3 Sensitivity calculation for cobalt gate electrode for sensing ammonia gas

$\Delta\ \phi_m(meV)$	I_{doff}(A/μm)	I_{don}(A/μm)	I_{don}/I_{doff}	S_{doff}
Without gas	8.21E-09	0.000526	64,026.2	1.00E+00
50	1.23E-09	0.000491	399,555	6.68E+00
100	1.83E-10	0.000455	2.49E+06	4.48E+01
150	2.72E-11	0.000418	1.54E+07	3.02E+02
200	4.02E-12	0.00038	9.45E+07	2.04E+03

Table 4 Sensitivity calculation for palladium gate electrode for sensing hydrogen gas

$\Delta\ \phi_m(meV)$	I_{doff}(A/μm)	I_{don}(A/μm)	I_{don}/I_{doff}	S_{doff}
Without gas	4.02E-12	0.00038	9.45E+07	1.00E+00
50	5.93E-13	0.000341	5.75E+08	6.77E+00
100	8.75E-14	0.000302	3.45E+09	4.59E+01
150	1.30E-14	0.000263	2.02E+10	3.09E+02
200	2.04E-15	0.000225	1.10E+11	1.97E+03

4 N + sige delta-doped gate stacked JL-VTFET features and working

Gas sensors function by converting the gaseous concentrations of various gases into electrical signals using specific chemical and physical effects. The gases, such as H_2 and NH_3, bind with the surface of gate contacts made up of catalytic metals; this changes the work function of the gate. Equation (1) affects the work feature variability due to pernicious gas molecule adsorption [16]. Where R stands for the gas constant, T stands for absolute temperature, and F and P stands for Faraday's constant and partial pressure. This system can be calibrated in terms of the gas's mole fractions in the air using the relational dependence of a gas's partial pressure on its concentrations. V_{fb}'s reliance on WFV is defined by Eq. (2) [25].

$$V_{fb} = \phi_m - \phi_s \pm \Delta\phi_m \tag{2}$$

where ϕ_s represents the work function of silicon, ϕ_m implies the work function of the metal.

However, for the employing variation in the gate metal work function, delta symbol is used $\Delta\phi_m$.

$$\phi_s = \frac{E_g}{2} + \chi - q\phi_{fp} \tag{3}$$

For N-channel, the OFF-state (I_{doff}) current alters by the proportionate change in the subthreshold slope, which leads to the shift in subthreshold voltage i.e. $V_{th.}$

$$I_{subthreshold} = I_0\left[e^{\frac{V_{gs}-V_{th}}{\eta V_{th}}}\right]\left[1 - e^{\frac{-V_{ds}}{V_{th}}}\right] \tag{4}$$

where

$$I_o = \frac{w\mu_n C_{ox} V_T^2 e^{1.8}}{L} V_T \tag{5}$$

V_{gs}, V_{ds}, and V_T represent the device's operating voltages, i.e., gate-source voltage, drain-source voltage, and thermal voltage, respectively. The transistor's effective width and length are denoted by L and w, respectively. C_{ox} stands for gate oxide capacitance, η stands for subthreshold swing

coefficient, and μ_n stands for electron mobility. As a result, the above equations define the relationships among the work function variation, threshold voltage (V_{th}), and transistor currents. The curves of surface potential, electric field, and energy band features are used to investigate the conduction behavior of the proposed JL-VTFET.

Figure 4a–c represents the variation of work function with the values of 50 meV, 100 meV, 150 meV, and 200 meV on the drain current (I_{ds}) for gate metal Molybdenum, Cobalt and Palladium, respectively. In order to drive drain current, one has used the proposed device of the N + SiGe gate staked JL-VTFET as a transducer. The reaction of gaseous molecules to the metallic surface is reflected by a commensurable electrical signal, i.e., in terms of variation in the I_{ds} current. From the graph outcomes, it can be analyzed that there is a large variation in the OFF-state current comparatively to the ON-state current. As a result, an exponentially decrement of the OFF-current will actually increase the sensitivity in the subthreshold regime, as can be verified using Eq. (6) [31]. Tunneling from band-to-band (BTBT) is strictly limited to thin channel and source boundaries [33].

$$S_{Idoff} = \frac{I_{doff(with\ out\ gas)}}{I_{doff(with\ gas)}} \tag{6}$$

Figure 3b shows the distribution of electron current density (A/cm^2) distribution of the proposed structure. From the color code, it can be analyzed that the red color is having the highest value in comparison to the purple color. However, this contour plot reflects the most of the concentration that lies at the source-channel junction by ranging with green color. It is evident from Fig. 3b that the electrostatic potential rises due to rise in the electron current density near the source-channel interface. It happens due to the high electrostatic control of the gate metal electrode over the channel.

Moreover, the variations in the work function will cause a change in the subthreshold voltage as the vertical TFETs are less resistant to the work function of the metal electrodes. (The calculations for sensitivity are given in Tables 2, 3, 4).

Figure 5a shows the proportionate variation of the electric field with reference to the work function. As the work function increases due to different metal catalysts, the greater value of the electric field is recorded. This happens due to a mitigation in the mobility of the charge carriers through the channel [32]. The gradient product of the electron density of states and the Fermi–Dirac distribution function defines the electric field. The electric field value increases steadily in the drain field, resulting in a persistent, slowly decreasing slope in the curve of the surface potential, as shown in Fig. 5b. Here, the electric field is represented as a function of the Fermi–Dirac distribution with electron density. Figure 5c shows how energy band diagrams evolve. Palladium

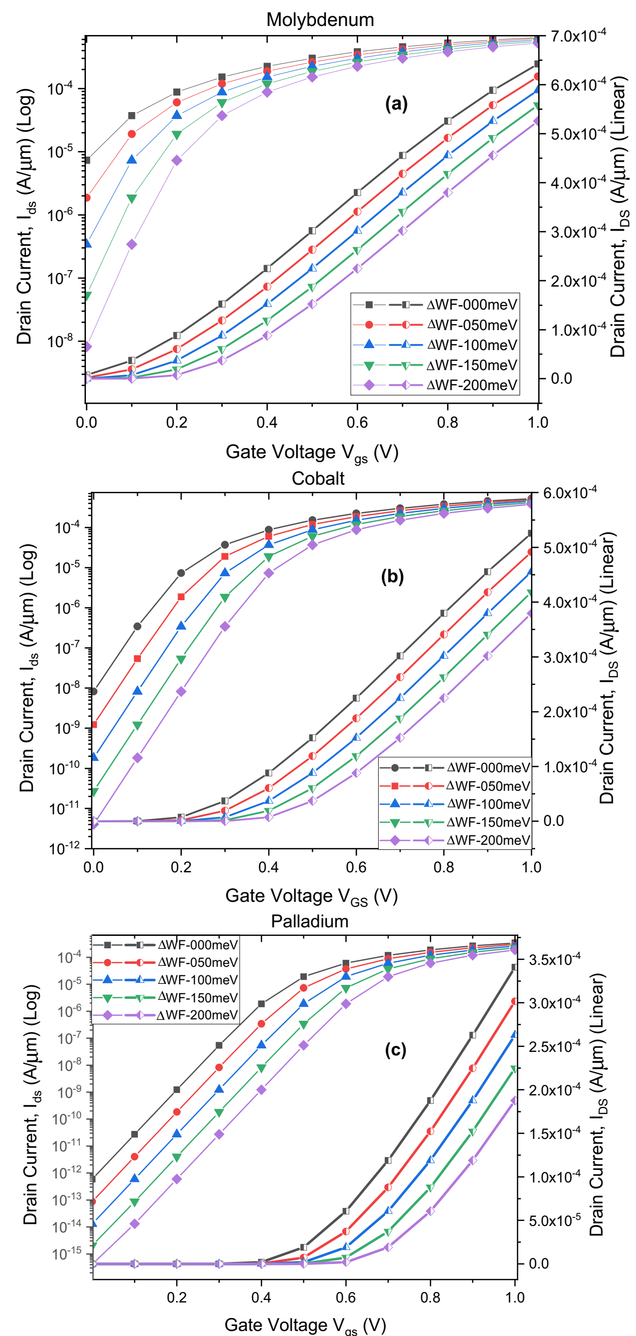

Fig. 4 Variation of drain current characteristics (I_{doff}) of the N + SiGe gate staked JL-VTFET with respect to the presence and absence of gas molecules for **a** Molybdenum **b** Cobalt **c** Palladium

has the highest tunneling barrier than Cobalt and Molybdenum since the work feature at the gate electrode is the highest. Furthermore, extra n-type charge carriers are drawn to the drain-side due to a higher drain bias. Figure 5d, e both indicate the valence band energy (eV) and conduction band energy (eV), 2D contour diagram, from which it can be concluded that energy at the control gate enables the electron to

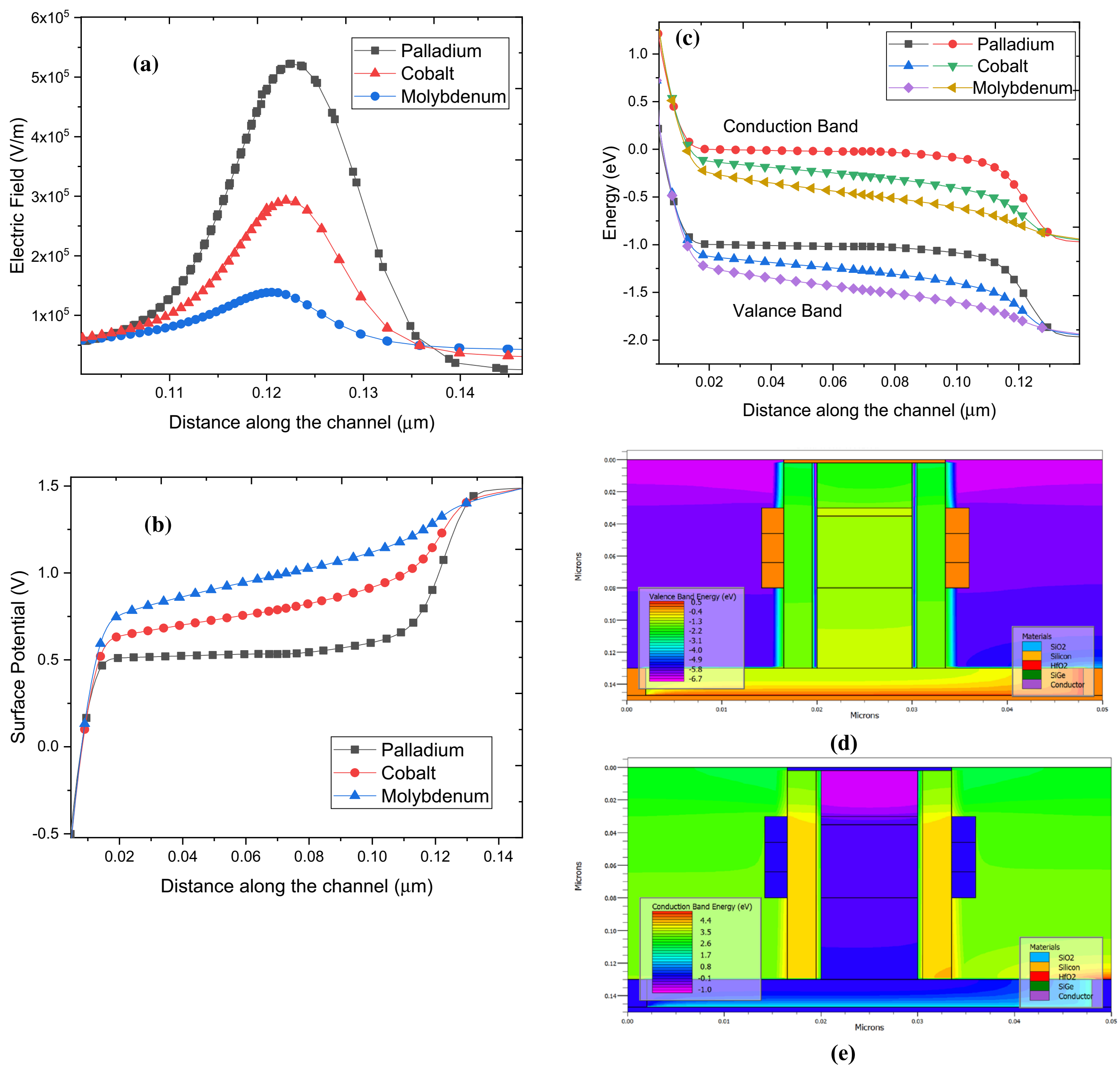

Fig. 5 **a** Electric field, **b** surface potential, **c** energy band diagram variation, **d** 2D contour plots of valence band energy distribution and **e** 2D contour plots of conduction band energy distribution of N + SiGe gate staked JL-VTFET with respect to different metal Molybdenum, Cobalt, Palladium work function at $V_{gs} = 1$ V and $V_{ds} = 1$ V

be transported from source to drain region. It is also evident from the graph that the concentration of electrons will also decrease moving towards the drain side. Similarly, the holes will be accumulated near the source region due to high work function (5.93 eV) as it is considered to be p-type in vertical tunneling, the energy band will be pulled down with the increase in the work function.

Now the next Figs. 6, 7 reflect the electric field and surface potential combined with respect to the work function variation (WFV) for the catalyst metal Molybdenum, Cobalt and Palladium, respectively. It can be directly observed from Fig. 6 that the electric field is directly proportionate to the work function value, as the WFV ($\Delta\phi_m$) increases, the electric field also increases. It shows sharp edges at the interface of the source-channel due to the presence of a delta-doping layer which increases the transmission of the charge carriers due to bandgap lowering at the tunneling junction.

Consequently, in Fig. 7a–c, the variation of the surface potential will look slightly in inverse relationship to the WFV. The bulk charge carriers will declare themselves to

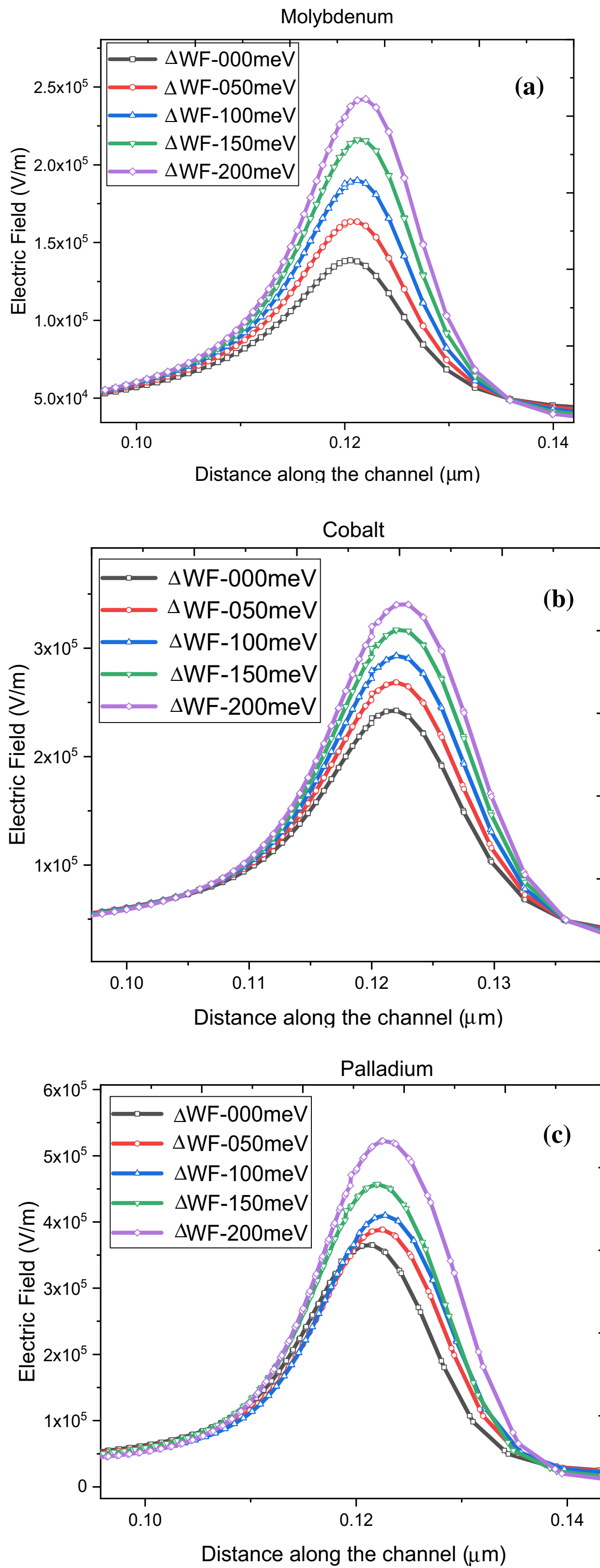

Fig. 6 Variation of electric field of the N + SiGe gate staked JL-VTFET with respect to the presence and absence of gas molecules (WFV) for **a** Molybdenum **b** Cobalt **c** Palladium

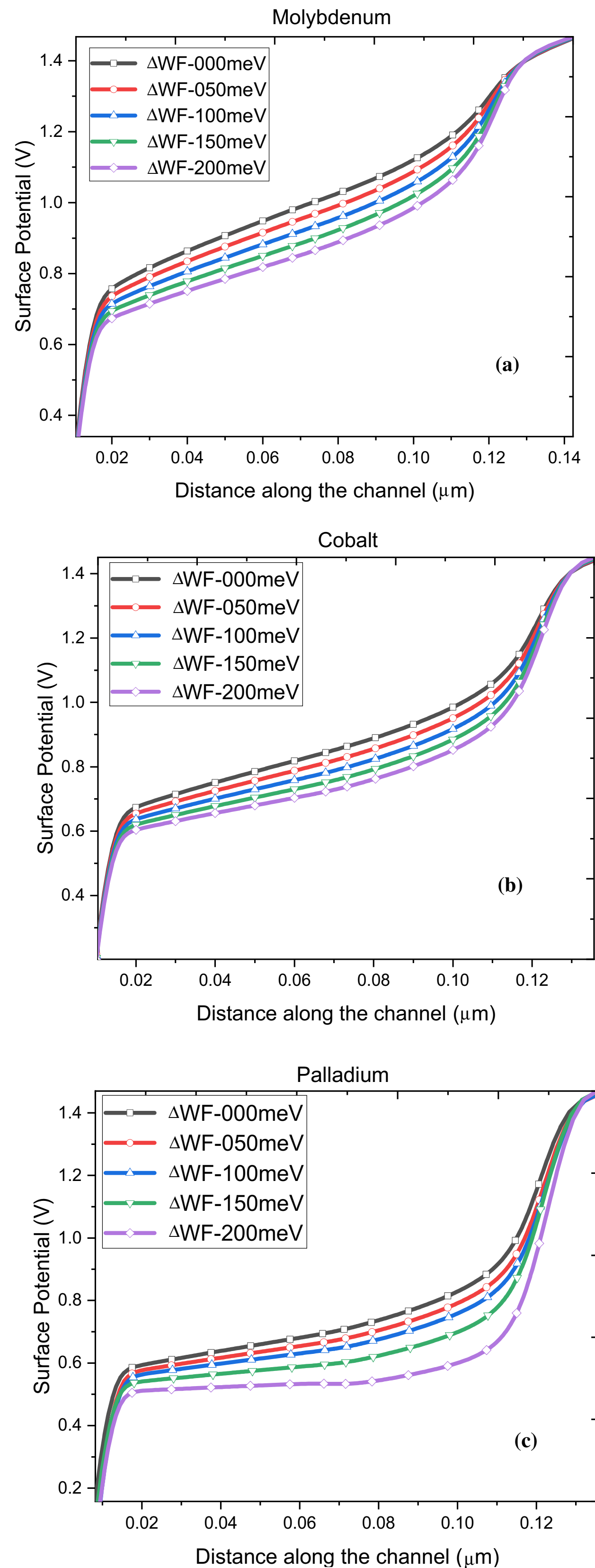

Fig. 7 Variation of Surface potential of the N + SiGe gate staked JL-VTFET with respect to the presence and absence of gas molecules (WFV) for **a** Molybdenum **b** Cobalt **c** Palladium

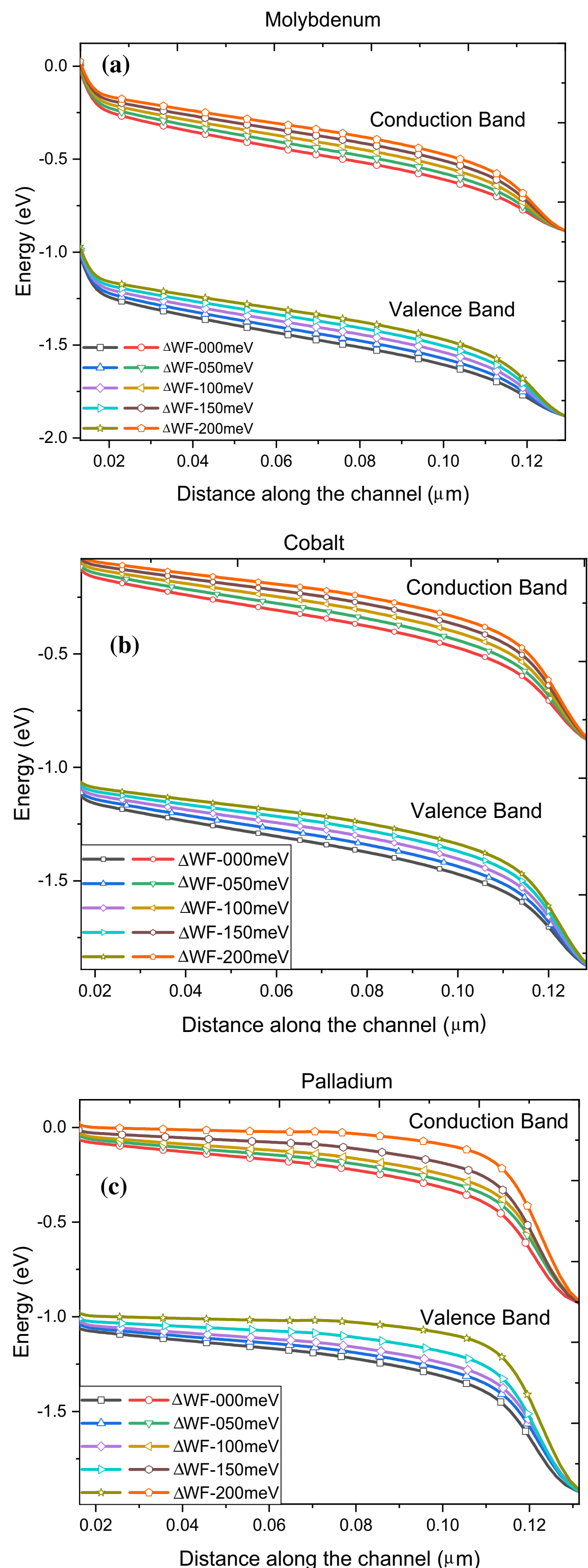

Fig. 8 Variation of energy band diagram of the N+SiGe gate staked JL-VTFET with respect to the presence and absence of gas molecules (WFV) for **a** Molybdenum **b** Cobalt **c** Palladium

be of p-type, which as a result will create a barrier to the tunneling current, and overall, the surface potential decreases [25]. The electric field reaches its highest value through the channel as we travel along the length of the unit. Therefore, the surface potential is considered to be the negative integral of the electric field.

Figure 8a–c depicts the shift of energy band diagrams as the work function increases. Palladium has the highest tunneling barrier (Fig. 5a) due to the highest value of work function at the gate electrode. Furthermore, due to a greater drain bias extra n-type charge carriers are attracted to the drain-side. Cumulative effect is depicted in Fig. 5a as individual peak formation for the given gate-metal-electrode. The increased work mechanism causes a higher concentration of p-type to form, which is the primary cause of energy band shifts. Additionally, p+pockets induced near the source-channel interface promote increased tunneling than near the drain region due to the elevated work function (5.93 eV) applied to the source terminal. Compared to source-channel space, the increased tunneling initiates in an extended bandgap close to the drain area, as seen in the graphs.

5 Result and discussion

In this section, the role of N+SiGe gate staked JL-VTFET is shown as a transducer. From Fig. 3a, one can easily analyze the comparison with the referenced structure [30], as the ON-state current is quite high. In contrast to earlier gas sensor designs, the sensitivity values for JT-VTFET-based sensors using Co, Mo, and Pd metals as gate contacts are much higher. The variation of different metals as gate electrodes is shown here as a function of the non-local band-to-band tunneling for electrons and holes along with the electron and holes concentration at the source-channel interface.

Figure 9a represents the non-local band to band tunneling rate for electrons with respect to the metal gate electrode of Molybdenum, Cobalt and Palladium. It can be clearly seen from the figure that with increase metal gate electrode the graph state increases near the source-channel interface due to the presence of the SiGe layer, which lowers the energy bandgap at the tunneling junction and increases the electrostatic control over the device channel. However, Fig. 9b shows the inverse relationship to Fig. 9a. The hole non-local BTBT will start decreasing the slope with respect to an increase in the gate metal electrode.

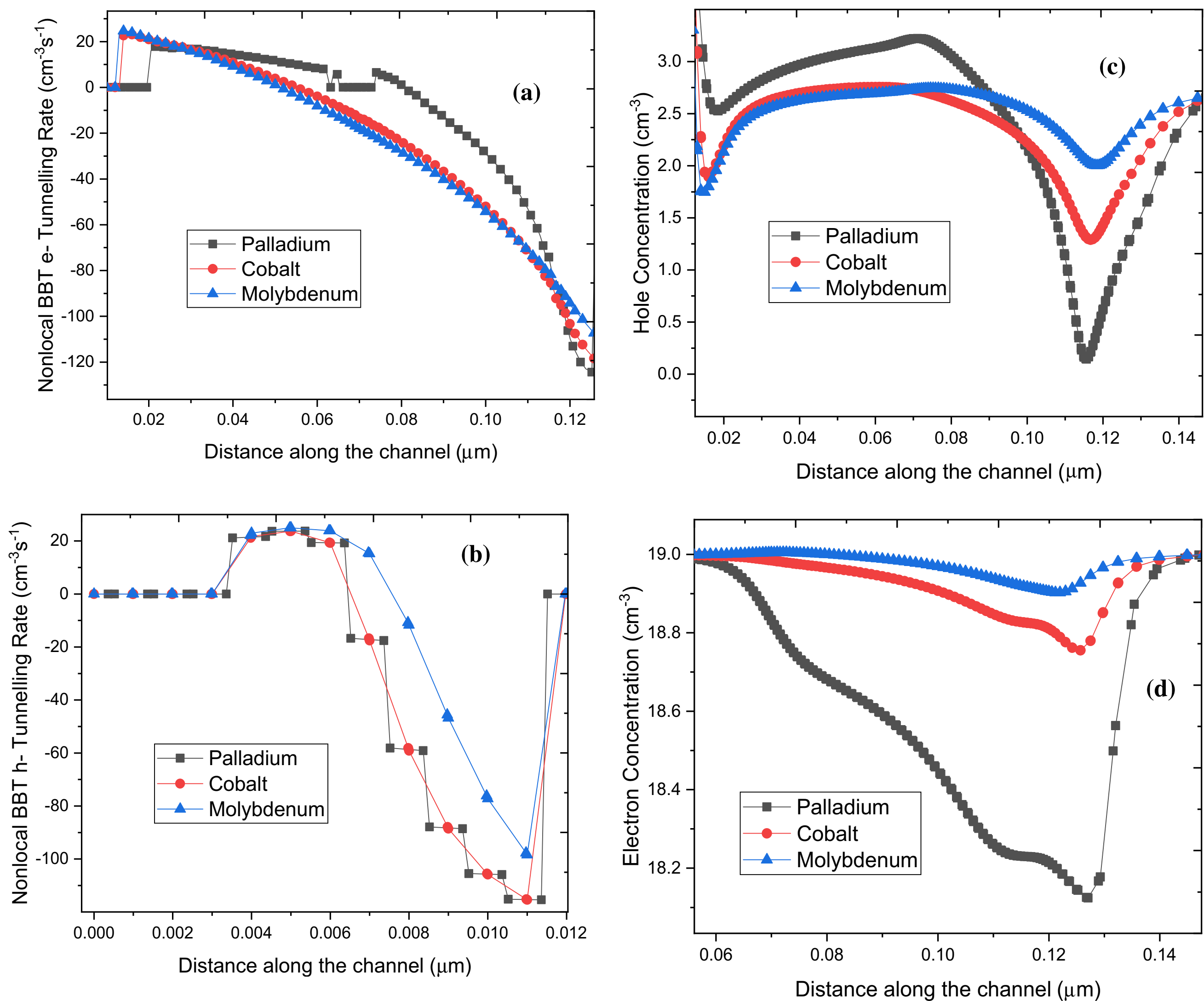

Fig. 9 Analysis of **a** non-local BBT e- Tuneling Rate (cm^{-3} s^{-1}) **b** non-local BBT e- Tuneling Rate (cm^{-3} s^{-1}) **c** Hole Concentration (cm^{-3}) **d** Electron concentration (cm^{-3}) for the N + SiGe gate staked JL-VTFET with respect gate metal electrode of Molybdenum, Cobalt and Palladium

Additionally, Fig. 9c and Fig. 9d show the charge carrier of hole and electron distribution in a vertically downward direction from source to drain. From Fig. 9c it can be noticed that the concentration of holes suddenly starts decreasing at the source-channel interface and higher at the drain side. This happens due to hole concentration higher at the drain side, which will control the device ambipolarity. However, in Fig. 9d shows the small piece of vicinity near the source side due to the presence of SiGe layer at the source-channel interface [30].

Figure 10a reflects the ON/OFF current ratio with respect to metal gate electrodes for Molybdenum, Cobalt, and Palladium. This graph clearly shows the inverse linear relation to the variation of the high work function to the current ratio. As the work function increases with the larger value than ON/OFF current, having the less ratio among them, i.e., it will overall decrease. However, Fig. 10b shows the variation of deriving sensitivity using Eq. (6) with respect to metal gate electrodes for Molybdenum, Cobalt, and Palladium. It can be reported from Table 2,3,4 that the derived sensitivity is higher for the lower work function, i.e., for Molybdenum, Cobalt, and Palladium, it is 8.89×10^2, 2.04×10^3, and 1.97×10^3, respectively. This happens due to less effect on the potential barrier at the source-channel interface due to the presence of the SiGe Layer [26]. So, we can conclude that, with the decrease in the OFF current, the sensitivity will increase.

For continuous monitoring of the surrounding gas atmosphere, long-time stability of the gas sensor is required. Furthermore, in many applications, quick sensor response and

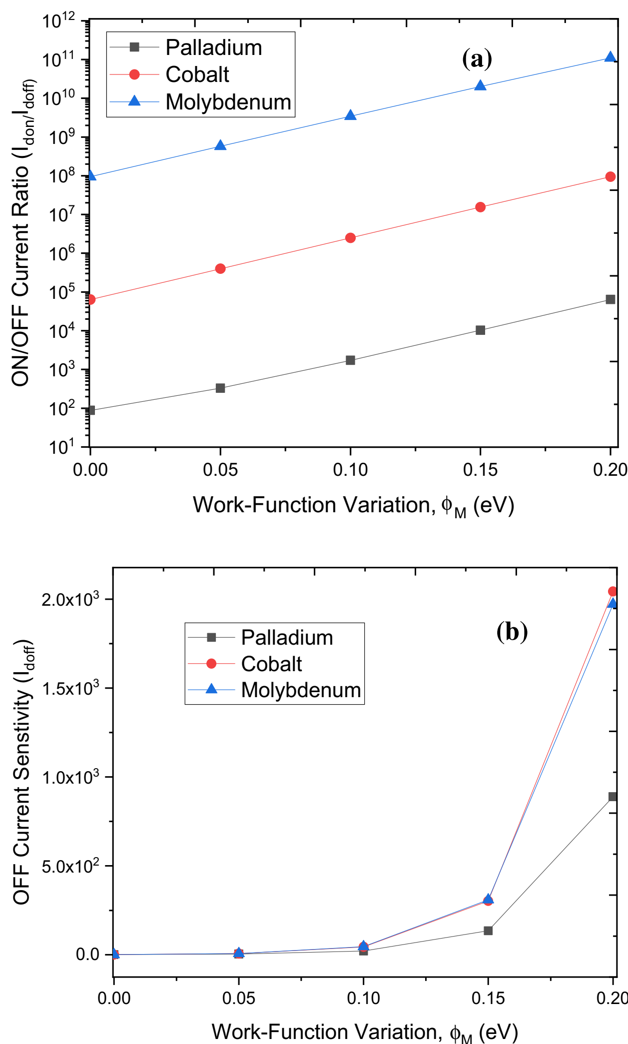

Fig. 10 Variation of **a** ON/OFF current **b** OFF current sensitivity (S_{Idoff}) of the N+SiGe gate staked JL-VTFET with respect to metal gate electrode for Molybdenum, Cobalt, and Palladium

recovery time are required, particularly for hazardous gas detection [34–36]. As response time is basically the time interval required by the sensor resistance to change from initial to final value almost 90% when exposed to analyzing gas, and recovery time is the time interval required by the sensor resistance (almost 10%) to retain its original value after the removal of the analyzing gas. Many studies in the field of material science have presented their coated thin film to a gas sensing chamber to calculate its response and recovery time in order to improve stability [37]. However, this parameter will be calculated after fabricating the device to the circuit level that will be exposed with the given concentrations of the gas molecules which will change the device work function (sensor resistance) for a certain time interval.

6 Conclusion

This literature has applied the concept of a single metal gate junctionless Vertical TFET as a gas sensor with high sensitivity. Palladium, a strongly reactive catalytic metal, has a sensitivity of 9.69×10^3 for sensing of Ammonia gas, whereas Molybdenum and Cobalt as gate contacts have a sensitivity of 8.89×10^2 and 1.97×10^3, respectively, for a sleek improvement in the value of 200 meV work function, demonstrating the efficiency of suggested design. The I_{don}/I_{doff} ratios obtained indicate that the proposed structure is a good choice. With respect to gate design and channel-related factors, further optimization is possible. Studying system behavior in the subthreshold slope regime provides the potential for increased sensitivity in order to introduce a cost-efficient, low-power gas detector with a reduced on-chip field. JL-VTFET is a potential choice for new research on gas sensing applications due to its vertical design, improved gate controllability, and lack of a sharp doping gradient.

References

1. D.J. Frank, R.H. Dennard, E. Nowak, P.M. Solomon, Y. Taur, H.-S. Wong, Device scaling limits of Si MOSFETs and their application dependencies. Proc. IEEE **89**(3), 259–288 (2001)
2. S.O. Koswatta, M.S. Lundstrom, D.E. Nikonov, Performance comparison between pin tunneling transistors and conventional MOSFETs. IEEE Trans. Electron Devices **56**(3), 456–465 (2009). https://doi.org/10.1109/TED.2008.2011934
3. S. Singh, B. Raj, Analytical modelling and simulation of Si-Ge hetero-junction dual material gate vertical T-shaped tunnel FET. SILICON **13**, 1139–1150 (2021)
4. Y. Khatami, K. Banerjee, Steep Subthreshold Slope n- and p-Type Tunnel-FET devices for low-power and energy-efficient digital circuits. IEEE Trans. Electron Devices **56**(11), 2752–2760 (2009). https://doi.org/10.1109/TED.2009.2030831
5. Singh, Shailendra, and Balwinder Raj (2020). Analysis of ONOFIC technique using SiGe heterojunction double gate vertical TFET for low power applications. Silicon: 1–10.
6. S. Singh, B. Raj, Modeling and simulation analysis of SiGe heterojunction double gate vertical t-shaped tunnel FET. Superlattices Microstruct. **142**, 106496 (2020)
7. Krishnamohan, Tejas, Donghyun Kim, Shyam Raghunathan, and Krishna Saraswat. "Double-Gate Strained-Ge Heterostructure Tunneling FET (TFET) With record high drive currents and≪ 60mV/dec subthreshold slope." In *2008 IEEE International Electron Devices Meeting*, pp. 1–3. IEEE, 2008. DOI: https://doi.org/10.1109/IEDM.2008.4796839
8. Gupta, Shilpi, Subodh Wairya, and Shailendra Singh (2021). Design and Analysis of Triple Metal Vertical TFET Gate Stacked with N-Type SiGe Delta-Doped Layer. Silicon. 1–9.
9. E.-H. Toh et al., Device physics and design of germanium tunneling field-effect transistor with source and drain engineering for low power and high-performance applications. J. Appl. Phys. **103**(10), 104504 (2008)
10. S. Singh, B. Raj, Two-dimensional analytical modeling of the surface potential and drain current of a double-gate vertical

t-shaped tunnel field-effect transistor. J. Comput. Electron. **19**(3), 1154–1163 (2020)
11. H. Damrongplasit, S.H. Nattapol, Kim, and Tsu-Jae King Liu, Study of random dopant fluctuation induced variability in the raised-Ge-source TFET. IEEE Electron Device Lett. **34**(2), 184–186 (2013)
12. W.V. Devi, B. Bhowmick, Optimisation of pocket doped junctionless TFET and its application in digital inverter. Micro Nano Lett. **14**(1), 69–73 (2019)
13. G.L. Priya, N.B. Balamurugan, New dual material double gate junctionless tunnel FET: Subthreshold modeling and simulation. AEU-Int. J. Electron. Commun. **99**, 130–138 (2019)
14. Singh, Shailendra, and Balwinder Raj (2020). Study of parametric variations on hetero-junction vertical t-shape TFET for suppressing ambipolar conduction.
15. Brinker, C. Jeffrey, and George W. Scherer (2013). Sol-gel science: the physics and chemistry of sol-gel processing. Academic press.
16. G.F. Fine, L.M. Cavanagh, A. Afonja, R. Binions, Metal oxide semiconductor gas sensors in environmental monitoring. Sensors **10**(6), 5469–5502 (2010)
17. J. Wöllenstein, M. Burgmair, G. Plescher, T. Sulima, J. Hildenbrand, H. Böttner, I. Eisele, Cobalt oxide-based gas sensors on silicon substrate for operation at low temperatures. Sens. Actuators, B Chem. **93**(1–3), 442–448 (2003)
18. D. López-Torres, A. Lopez-Aldaba, C.E. Aguado, J.-L. Auguste, R. Jamier, P. Roy, M. López-Amo, F.J. Arregui, Sensitivity optimization of a microstructured optical fiber ammonia gas sensor by means of tuning the thickness of a metal oxide nano-coating. IEEE Sens. J. **19**(13), 4982–4991 (2019)
19. B. Timmer, W. Olthuis, A. Van Den Berg, Ammonia sensors and their applications—a review. Sens. Actuators, B Chem. **107**(2), 666–677 (2005)
20. K. Tsukada, M. Kariya, T. Yamaguchi, T. Kiwa, H. Yamada, T. Maehara, T. Yamamoto, S. Kunitsugu, Dual-gate field-effect transistor hydrogen gas sensor with thermal compensation. Japanese J. Appl. Phys. **49**(2R), 024206 (2010)
21. D. Connelly, D.E. Carl Faulkner, Grupp, and J. S. Harris, , A new route to zero-barrier metal source/drain MOSFETs. IEEE Trans. Nanotechnol. **3**(1), 98–104 (2004)
22. Semiconductor Industry Association (SIA), International Technology Roadmap for Semiconductors (ITRS), 2015.
23. Manual, Atlas Users. "Device simulation software, Silvaco Int." Santa Clara, CA, Version 5, no. 0 (2010).
24. S. Singh, B. Raj, Analytical modeling and simulation analysis of T-shaped III-V heterojunction vertical T-FET. Superlattices Microstruct. **147**, 106717 (2020)
25. S. Singh, M. Khosla, G. Wadhwa, B. Raj, Design and analysis of double-gate junctionless vertical TFET for gas sensing applications. Appl. Phys. A **127**(1), 1–7 (2021)
26. S. Singh, B. Raj, Design and analysis of a heterojunction vertical t-shaped tunnel field effect transistor. J. Electron. Mater. **48**(10), 6253–6260 (2019)
27. Loubet, N., T. Hook, P. Montanini, C-W. Yeung, S. Kanakasabapathy, M. Guillom, T. Yamashita et al. "Stacked nanosheet gate-all-around transistor to enable scaling beyond FinFET." In 2017 Symposium on VLSI Technology, pp. T230-T231. IEEE, 2017.
28. A. Bhattacharyya, M. Chanda, D. De, Performance assessment of new dual-pocket vertical heterostructure tunnel FET-based biosensor considering steric hindrance issue. IEEE Trans. Electron Devices **66**(9), 3988–3993 (2019)
29. P.K. Dubey, B.K. Kaushik, T-shaped III-V heterojunction tunneling field-effect transistor. IEEE Trans. Electron Devices **64**(8), 3120–3125 (2017)
30. N. Jayaswal, A. Raman, N. Kumar, S. Singh, Design and analysis of electrostatic-charge plasma based dopingless IGZO vertical nanowire FET for ammonia gas sensing. Superlattices Microstruct. **125**, 256–270 (2019)
31. M. Verma, S. Tirkey, S. Yadav, D. Sharma, D.S. Yadav, Performance assessment of a novel vertical dielectrically modulated TFET-based biosensor. IEEE Trans. Electron Devices **64**(9), 3841–3848 (2017)
32. W.V. Devi, B. Bhowmick, P.D. Pukhrambam, N+ pocket-doped vertical TFET for enhanced sensitivity in biosensing applications: modeling and simulation. IEEE Trans. Electron Devices **67**(5), 2133–2139 (2020)
33. S. Shailendra, B. Raj, Analytical and compact modeling analysis of a SiGe hetero-material vertical L-shaped TFET. Silicon, pp. 1–11 (2021)
34. R. Gautam, R.S. Manoj Saxena, Gupta and Mridula Gupta, , Gate-all-around nanowire MOSFET with catalytic metal gate for gas sensing applications. IEEE Trans. Nanotechnol. **12**(6), 939–944 (2013)
35. M. Safari, M. Gholizadeh, A. Salehi, Modeling and simulation of a MOSFET gas sensor with platinum gate for hydrogen gas detection. Sens. Actuators, B Chem. **141**(1), 1–6 (2009)
36. Dan, Yaping, Stephane Evoy, and A. T. Johnson. "Chemical gas sensors based on nanowires." arXiv preprint http://arxiv.org/abs/0804.4828 (2008).
37. B. Karunagaran, S.J. Periyayya Uthirakumar, S.V. Chung, E.-K. Suh, TiO2 thin film gas sensor for monitoring ammonia. Mater. Charact. **58**(8–9), 680–684 (2007)

Publisher's Note Springer Nature remains neutral with regard to jurisdictional claims in published maps and institutional affiliations.